HHS Public Access

Author manuscript

J Cell Biochem. Author manuscript; available in PMC 2017 August 11.

Published in final edited form as:

J Cell Biochem. 2017 May ; 118(5): 1038–1049. doi:10.1002/jcb.25673.

Characterization of Laminin Binding Integrin Internalization in Prostate Cancer Cells†

Lipsa Das[1], **Todd A. Anderson**[6], **Jaime M.C. Gard**[6], **Isis C. Sroka**[2], **Stephanie R. Strautman**[5], **Raymond B. Nagle**[4,6], **Colm Morrissey**[7], **Beatrice S. Knudsen**[8], and **Anne E. Cress**[3,5,6,*]

[1]Department of Cancer Biology, University of Arizona, Tucson, AZ 85724

[2]Department of Pharmacology, University of Arizona, Tucson, AZ 85724

[3]Department of Cellular and Molecular Medicine, University of Arizona, Tucson, AZ 85724

[4]Department of Pathology, University of Arizona, Tucson, AZ 85724

[5]Department of Molecular and Cellular Biology, University of Arizona, Tucson, AZ 85724

[6]The University of Arizona Cancer Center, University of Arizona, Tucson, AZ 85724

[7]University of Washington, Seattle WA 98195

[8]Cedars Sinai Medical Center, Los Angeles, CA 90048

Abstract

Laminin binding integrins α6 (CD49f) and α3 (CD49c) are persistently but differentially expressed in prostate cancer (PCa). Integrin internalization is an important determinant of their cell surface expression and function. Using flow cytometry, and first order kinetic modelling, we quantitated the intrinsic internalization rates of integrin subunits in a single cycle of internalization. In PCa cell line DU145, α6 integrin internalized with a rate constant (k_{actual}) of 3.25min^{-1}, 3-fold faster than α3 integrin (1.0 min^{-1}), 1.5-fold faster than the vitronectin binding αv integrin (CD51) (2.2 min^{-1}), and significantly slower than the unrelated transferrin receptor (CD71) (15 min^{-1}). Silencing of α3 integrin protein expression in DU145, PC3 and PC3B1 cells resulted in up to a 1.71-fold increase in k_{actual} for α6 integrin. The internalized α6 integrin was targeted to early endosomes but not to lamp1 vesicles. Depletion of α3 integrin expression resulted in redistribution of α6β4 integrin to an observed cell-cell staining pattern that is consistent with a suprabasal distribution observed in epidermis and early PIN lesions in PCa. Depletion of α3 integrin increased cell migration by 1.8 fold, which was dependent on α6β1 integrin. Silencing of α6 integrin expression however, had no significant effect on the k_{actual} of α3 integrin or its distribution in early endosomes. These results indicate that α3 and α6 integrins have

†This article has been accepted for publication and undergone full peer review but has not been through the copyediting, typesetting, pagination and proofreading process, which may lead to differences between this version and the Version of Record. Please cite this article as doi: [10.1002/jcb.25673]

*Corresponding Author: Anne E. Cress, Department of Cellular and Molecular Medicine, The University of Arizona Cancer Center, 1515 N. Campbell Ave., Tucson, AZ 85724, USA, Tel: (520) 626-7553, Fax: (520) 626-4979, cress@email.arizona.edu.

Additional Supporting Information may be found in the online version of this article.

The authors declare no conflicts of interest.

significantly different internalization kinetics and that coordination exists between them for internalization. This article is protected by copyright. All rights reserved

Keywords

integrin; laminin; internalization kinetics; endosomes; prostate cancer

Integrins are cell surface receptors involved in cell matrix adhesion, signaling, and cell migration [Hood and Cheresh, 2002; Sroka et al., 2010; Watt, 2002]. The laminin binding integrins (α3 and α6 containing heterodimers; α3β1, α6β1, and α6β4) represent a conserved class of integrins essential for the normal development of vertebrate and non-vertebrate life forms [Frank and Miranti, 2013; Hynes, 2002; Longmate and Dipersio, 2014; Marchetti et al., 2013]. For simplicity, α6β1 and α6β4 integrins will be referred to here as α6 integrin. Integrins α3 and α6 function coordinately during embryonic development [De Arcangelis et al., 1999; DiPersio et al., 1997] as well as in adult processes such as epithelial regeneration and wound healing [Longmate and Dipersio, 2014; Margadant et al., 2009]. Mice lacking the α6 integrin die shortly after birth because of severe blistering of the skin and other epithelia [Georges-Labouesse et al., 1996], a defect that can only be partially compensated by α3 integrin [De Arcangelis et al., 1999; van der Neut et al., 1996]. During development and wound healing, both of these integrins show an orchestrated redistribution of their cellular localization that affects their function [Shimizu et al., 2012]. During cell migration, α3 integrin [Barczyk et al., 2010] is observed at the tip of the lamellipodia and is involved in the deposition of a provisional extracellular matrix, subsequently utilized by α6 integrin for collective epithelial migration [Margadant et al., 2009].

In humans, α3 and α6 integrins are expressed in various epithelial cancers [Desgrosellier and Cheresh, 2010; Stipp, 2010]. Only laminin binding integrins are detected in biopsy and prostatectomy specimens of primary prostate tumors, as well as in bone metastasis specimens [Schmelz et al., 2002], demonstrating a loss of the variety of integrin expression in prostate cancer as compared to normal glands [Cress et al., 1995]. Although the majority of prostate cancers (80%) express either/both α3 or α6 integrins on the tumor cell surface, 26% express only integrin α6 [Schmelz et al., 2002]. Additionally, the loss of surface α3 integrin expression positively correlated with high Gleason grade and the pathological stage of the cancer [Schmelz et al., 2002].

Likewise, expression of α6 integrin is an important determinant of tumor progression, reduced patient survival, and increased metastasis [Ports et al., 2009; Schmelz et al., 2002]. Integrin α6 is a marker of prostate cancer stem cells or tumor initiating cells [Park et al., 2016; Schmelz et al., 2005]. Previous work has shown a strong expression of α6 integrin during perineural invasion [Sroka et al., 2010] and bone metastasis in prostate cancer [Landowski et al., 2014; Schmelz et al., 2002]. A tumor-specific functional variant, α6p, is a key contributor to cancer metastasis [Demetriou and Cress, 2004; Demetriou et al., 2008; Ports et al., 2009]. However, the role of α3 integrin in cancer progression remains less clear [Stipp, 2010]. Several studies report α3 integrin is pro-metastatic [Mitchell et al., 2010; Zhou et al., 2014], while others have defined α3 integrin as a mediator of cell spreading and

a negative regulator of metastasis [Demetriou and Cress, 2004; Varzavand et al., 2013]. The coordination of α6 and α3 function on the cell surface may be an important factor to consider in evaluating α3 integrin function in cancer progression.

An important determinant of the cell surface expression and function of integrins is their intracellular trafficking. Cell surface integrins are internalized to early endosomes, where they can be recycled back to the membrane to promote cell migration or routed to the lysosome for degradation [Bridgewater et al., 2012; Ramsay et al., 2007]. RabGTPases control these specific trafficking pathways and are often deregulated in cancer [Goldenring, 2013]. Internalization and recycling of α6 integrin is reported to be crucial for migration of neuronal cells during development [Strachan and Condic, 2004] and in hypoxia-induced breast cancer invasion [Yoon et al., 2005]. Additionally, each alpha integrin is known to have a distinct internalization rate despite sharing the same β1 integrin partner [Bretscher, 1992].

In the present study, we characterized the internalization kinetics of laminin binding integrins and used it to determine if the differential expression of α3 and α6 integrin influenced respective internalization rates and intracellular localization. Receptor internalization can be influenced by ligand binding, integrin activation state, integrin clustering, membrane micro domain location, cell type, pH, and temperature [De Franceschi et al., 2015]. In order to minimize these variables, internalization rates were obtained using suspension cells as previously reported, to obtain “steady-state” or intrinsic internalization characteristics of the receptor being studied [Bretscher, 1992; Knauer et al., 1984]. Quantitation of the internalization kinetic parameters of the receptor(s) using flow cytometry and kinetic modeling [Wiley and Cunningham, 1982a] revealed that α3 integrin negatively influenced α6 integrin internalization. Depletion of α3 integrin expression increased trafficking of α6β4 integrin to early endosomes and resulted in the redistribution of α6β4 integrin to the membrane at cell-cell locations.

MATERIALS AND METHODS

Cells, Antibodies, and Reagents

Human prostate cancer cell lines DU145, PC3, LNCaP, VCaP, 22Rv1 and immortalized human keratinocyte cell line HaCaT were obtained from the American Type Tissue Collection (ATCC, Manassas, VA). Human PC3B1 prostate cancer cells were isolated from the bone marrow of SCID mice that had been injected six weeks previously with the PC3 cell line as described earlier [Ports et al., 2009]. Each prostate cancer cell line was cultured in Iscove’s modified Dulbecco’s medium (IMDM) from Invitrogen (Grand Island, NY) supplemented with 10% fetal bovine serum (FBS) Hyclone Laboratories (Novato, CA) at 37 °C in a 5% CO_2. Trypsin-EDTA (Gibco, NY) or non-enzymatic Cellstripper (CellGro, Manassas, VA) were used to obtain adherent cells. HaCaT were grown in Dulbecco’s medium (Invitrogen, Grand Island, NY) +10% FBS and the conditioned media enriched in laminin-511 and laminin-332, as reported [Sroka et al., 2008] was harvested.

Fluorophore conjugated antibodies used for flow cytometry include: phycoerythrin (PE) conjugated GoH3 (eBioscience, San Diego, CA) against α6 integrin; fluorescein-conjugated P1B5 (R&D Systems, Minneapolis, MN) against α3 integrin; FITC conjugated TS2/16

(eBiosciences) against-β1 integrin; Alexa Fluor 660 conjugated anti-β4 antibody (clone 439-9B, eBiosciences) and FITC conjugated anti-transferrin receptor CD71 antibody (eBiosciences)

Antibodies used for immunofluorescence staining include: anti-α6 integrin J1B5 rat monoclonal antibody, anti-α3 integrin P1B5 mouse monoclonal antibody (EMD Millipore, Massachusetts) and anti-β4 integrin ASC3 mouse monoclonal antibody (EMD Millipore). Antibodies against endocytic markers were FITC conjugated mouse anti-EEA1 (Early Endosome Antigen-1) antibody (BD transduction Laboratories), anti-rat Alexa 546 and anti-rabbit Alexa 633 conjugated secondary antibodies (Invitrogen, Carlsbad, CA). Anti-α6 integrin antibody AA6NT [Ports et al., 2009] and anti-α3 integrin antibody AB1920 (Chemicon, Temecula, CA), horseradish peroxidase–conjugated secondary antibodies (Jackson Immuno-Research Laboratories, Inc., West Grove, PA) were used for western blotting.

Anti-β1 integrin antibody AIIB2 (Developmental Studies Hybridoma Bank, University of IOWA, Iowa City, Iowa) was used for blocking adhesion function of the integrin. Laminin mimetic peptide HYD1 and a scrambled peptide, HYDS, were used as previously reported [Sroka et al., 2006].

Silencing expression by siRNA

DU145 cells (30% confluent) were treated with 25nM Dharmacon siRNA (Thermo Scientific, Lafayette, CO) specific for α6 or α3 integrin or with the non-targeting siRNA (SiGENOME Control Pool Non-Targeting #2) using DharmaFECT transfection reagent for 72 hours.

Flow cytometry internalization assay

DU145 cells were obtained with Cellstripper and washed with cold PBS (Phosphate buffer saline) containing 0.2% BSA. Cell surface receptors were labelled with fluorophore-conjugated antibodies specific for integrin subunits or transferrin receptor at 4°C for 45 minutes. Unbound antibody was removed with cold PBS. Cells were incubated in media supplemented with 10% FBS at 37°C for internalization, followed by stopping the reaction at 4°C. Antibody remaining at the cell surface was removed using cold acid solution (0.5M NaCl, 0.2M CH_3COOH) for 5 minutes followed by PBS wash. Cells were fixed in PBS containing 1% formaldehyde and analyzed using a FACScan (BD Biosciences, San Jose, CA). Internalized label for each time point was calculated as a percent of the full label mean peak fluorescence (MPF) value. At least three independent experiments were performed for each receptor. A first-order kinetics model was created using KaleidaGraph (Synergy Software) and provided a good fit for the receptor internalization kinetics ($R^2 > 0.98$) according to the following formula,

$$y=a+b[1-\exp(-k_{obs}t)],$$

where, y is the amount of receptor internalized at time t (in min), b is the maximum intracellular accumulation of the receptor, and k_{obs} is the observed first-order rate constant

(min^{-1}) [Wiley and Cunningham, 1982b]. Actual rate constant k_{actual} (= b*k_{obs}) was calculated as a measure of net internalization rate at the steady state of maximum internal accumulation. All values are reported as mean±standard error. Statistical analysis of the results was performed by Student's t test for unpaired samples. A P-value lower than 0.05 was considered statistically significant.

Cell migration assay

Cell migration was assessed using a modified Boyden chamber assay. Cell culture inserts (BD Biosciences, San Jose, CA, USA) of pore size 8 μm were coated on the underside with laminin enriched 50 μL HaCaT conditioned media overnight at 4°C. Approximately 15,000 cells (siRNA treated) in 200 μL IMDM were plated into the upper chamber of each insert. Function blocking anti-β1 integrin antibody AIIB2 (1 mg/ml; 1:100) was added to cells prior to plating. Inserts were placed into wells containing 600 μL IMDM plus 10% FBS in a 24-well tissue culture plate and incubated for 6 hours at 37°C in a humidified incubator. Cells on the underside of the insert were fixed/permeabilized in methanol/acetone and stained with 4′, 6-diamidino-2-phenylindole (DAPI) (1μg/mL) (Sigma Chemical Co., St. Louis, MO, USA) for nuclei detection. The cell numbers were counted in five sections of each insert (four corners and the middle) using the Zeiss Axiophot inverted fluorescent microscope at 20X magnification. Experiments were performed 3 times in triplicate, and the average number of cells per insert was calculated.

Immunofluorescence staining

DU145 cells grown to 70% confluence on glass coverslips were incubated with anti-α6 integrin antibody J1B5, anti-α3 P1B5 antibody or anti-β4 ASC3 antibody diluted to 1:100 IMDM+10% FBS media for 40 minutes in presence of 0.5 mM primaquine (Invitrogen, Carlsbad, CA), a recycling inhibitor. The cells were fixed using PBS containing 2% formaldehyde and permeabilized with PBS containing 0.2% Triton X-100. After blocking with 2% BSA for 20 minutes at room temperature, cells were incubated with antibodies against endocytic markers Alexa 488 conjugated mouse EEA1 (1:250) and Lamp1 (1:200) for 40 minutes. Cells were incubated with anti-rat or anti-mouse Alexa 546 and anti-rabbit Alexa 633 conjugated secondary antibodies for 30 minutes. Coverslips were mounted on slides using Prolong antifade (Invitrogen). Images were acquired using specimens were imaged using a DeltaVision Core system (GE Healthcare Bio-Sciences, Pittsburgh, United States of America) equipped with an Olympus IX71 microscope, a 60X objective (NA 1.20), and a cooled charge-coupled device camera (CoolSNAP HQ2; Photometrics). Single plane images were acquired and deconvolved with softWoRx v1.2 software (Applied Science). Images were analyzed using ImageJ plugin Just Another Colocalization Plugin (JACoP) to measure Pearson coefficient of co-localization (Pr) and percent endosomal vesicles positive for integrin.

RESULTS

Internalization rates of Integrin subunits

Internalization kinetics were quantified for the laminin binding α3 and α6 integrins, their binding partner β1 integrin, vitronectin binding αv integrin, and an unrelated abundant

transferrin receptor in DU145 cells. The general schema is shown (Fig. 1A). Since the cell surface receptors were labelled with fluorophore conjugated antibodies at 4°C, the internalization measured represents single cycle of internalization. Labelling of surface receptors was observed as an increase in mean peak fluorescence (MPF) values as compared to unlabeled cells (Fig. 1B, *left panel*). With increased time of internalization, the labelled cell surface receptor accumulated inside the cells, demonstrated by a gradual increase in the MPF values of the intracellular label (Fig. 1B, *right panel*). The percent of internalized surface label was calculated from MPF value of internalized label as compared to total surface label (Fig. 1C).

Significant α3 and α6 integrin internalization was observed within 10 minutes and approximately 40 to 60% of the label was internalized within one hour. Integrin α6 was internalized at a rate 3.25-fold higher than α3 integrin (k_{actual} = 3.25±0.16 min^{-1} and 1.00±.08 min^{-1} respectively, Fig. 1D). Intracellular accumulation of α6 integrin was ~2-fold higher than α3 integrin (58.09±0.85, 30.46±0.67 percent of total surface integrin, respectively). Integrin αv had a lower k_{actual} than α6 integrin but a higher intracellular accumulation (64.92±2.94). Transferrin receptor (TfR) was internalized with a significantly higher rate (k_{actual} = 15±4.60), at least 4 times that of α6 integrin.

Internalization kinetics of β1 integrin (Fig. 1C) revealed a maximal internalization of 75%, while 45% of surface β1 integrin was already internalized at 0 min. This was not surprising, as caveolin mediated internalization of β1 integrin has been reported to occur at 4°C [Goldfinger et al., 1999; Teckchandani et al., 2009]. Moreover, β1 integrin potentially has 11 alpha partners (α1–11), of which there is significant surface expression of α2, α3, α5, and α6 integrins in DU145 cells [Witkowski et al., 1993]. Thus, the β1 subunit internalized at 4°C may reflect a cumulative internalization of various β1 integrin containing heterodimers. Interestingly, the other beta partner of α6, the β4 integrin, was completely internalized at 4°C at 0 min in these cells (Fig. S1). This suggests that internalization rates of α6 subunit measured under a physiologically relevant temperature of 37°C were due to the α6β1 heterodimer.

Silencing α3 integrin expression increases internalization of α6 integrin

Since both α3 and α6 laminin binding integrin expression is preserved in the majority of human prostate cancer, experiments were designed to determine if their internalization kinetics were coordinated. The study was restricted to androgen receptor (AR) minus cell lines since AR positive cell lines (LNCaP, VCaP and 22Rv1) were negative for α3 integrin expression (Fig. S2). Three other prostate cancer cell lines were tested (DU145, PC3, PC3B1). Since they are AR negative, they represent advanced castration resistant prostate cancer and express both α3 and α6 integrin. The expression of α3 or α6 integrin was silenced (siα3 or siα6 cells respectively) and the effect on the internalization kinetics of the non-targeted integrin was determined. Importantly, silencing expression of either integrin did not have a measurable effect on the total cellular expression of the non-targeted integrin as seen by immunoblot analysis (Fig. 2A). Cell surface α6 integrin was labelled with PE-conjugated anti-α6 integrin antibody and a time-dependent increase in internalized label was observed. Representative flow profiles are shown for DU145 cells (Fig. 2B). In each of the

three cell lines, DU145, PC3, PC3B1, the internalization of α6 integrin in siα3 cells was significantly increased as compared to cells treated with non-targeting siRNA (siCON cells) (Fig. 2C). Kinetic rate constant analysis confirmed a statistically significant increase in k_{actual} of α6 integrin internalization as compared to siCON cells. DU145 cells showed 1.47 fold increase in k_{actual} (from 3.20min^{-1} to 4.72 min^{-1}), PC3 had a 1.71 fold increase (from 0.69 min^{-1} to 1.18 min^{-1}) PC3B1 had a 1.44 fold increase (from 1.04 min^{-1} to 1.47 min^{-1}) in siα3 cells versus siCON cells (Fig. 2D). The total intracellular accumulation, as judged by the amplitude of α6 integrin was increased in each of the three cell lines (52.48 to 63.83, 11.35% increase in DU145; 34.61 to 42.10, 7.49% increase in PC3; and 40.32 to 52.36, 12.04% increase in PC3B1 cells). Depletion of α3 integrin expression in all three cell lines increased the α6 integrin internalization rate up to 1.71 fold, despite the differences in the intrinsic α6 integrin internalization rates (Fig. 2C, D). These data showed that the observed increased α6 integrin internalization by α3 integrin depletion was independent of the intrinsic internalization rate.

Silencing α6 integrin expression does not affect internalization rate of α3 integrin

We next tested whether depletion of α6 integrin expression was a determining factor in α3 integrin internalization rates in the three cell lines DU145, PC3 and PC3B1. The silencing of α6 integrin (siα6) did not alter the total amount of α3 integrin expressed (Fig. 2A). The surface labelled α3 integrin internalized in a time dependent manner in siα6 or siCON cells as shown in representative flow cytometry profiles for the population of DU145 cells (Fig. 3A). Analysis of the MPF data obtained from the flow cytometry profiles generated the internalization curves (Fig. 3B). The internalization rate constant of α3 integrin was not significantly different in siCON and siα6 cells in any of the three cell lines. However, kinetic analysis predicted an increase in intracellular accumulation, as judged by an increase in amplitude (31.27 to 42.11; 11% increase) of α3 integrin in siα6 cells in DU145 cells (Fig. 3C). An increase in amplitude was also observed in PC3 (63.77 to 66.67; 3% increase) and in PC3B1 (51.84 to 62.18; 10% increase) (Fig. 3C). We note that while the three cell lines have similar intrinsic internalization rate constants for α3 integrin (DU145, PC3, PC3B1 rates were 1.03, 1.20, 1.19, respectively) a statistically significant difference exists in the total intracellular accumulation of the α3 integrin in DU145, PC3 and PC3B1 cells (31.27, 63.77 and 51.84, respectively).

A comparison of the actual rate constant of internalization (k_{actual}) of the laminin binding integrins and whether depletion of either alpha subunit affects the internalization of the other alpha subunit was tested in the three cell lines (Fig. 4). Silencing α3 integrin expression led to a statistically significant increase in internalization of the α6 subunit by 1.44–1.71-fold, but did not affect the k_{actual} of TfR internalization. The k_{actual} of α3 internalization remained unchanged on silencing α6 integrin expression.

We next tested whether a biologically active peptide called HYD1 or an antibody antagonist to α3 and α6 integrin function would alter internalization rates. HYD1 is a D-amino acid containing peptide that blocks α3 and α6 adhesion without altering signaling [Sroka et al., 2006] and AIIB2 will block β1 integrin adhesion function [Werb et al., 1989]. HYD1 did not affect the internalization of either α3 or α6 integrin (Fig. S3A). However, functional

blocking of their partner β1 integrin with the AIIB2 antibody reduced internalization of α6 integrin but not α3 integrin (Fig. S3B). These data further underscores the differential regulation of α3 and α6 internalization properties despite sharing the same β1 integrin partner.

Silencing α3 integrin expression increased α6β1 integrin dependent cell migration

The functional consequence of the increased α6 internalization rate was tested using a modified Boyden chamber migration assay. In brief, cells were plated on the top of the insert and allowed to migrate to the other side of the membrane, which was coated with laminin. Silencing expression of α3 integrin (siA3) resulted in a marked increase in cell migration as compared to the untreated (siCON) cells (1.8 fold, $^{**}p < 0.005$ Fig. 5, black bars). The increased cell migration induced by silencing of α3 (siα3) was dependent upon α6 integrin since dual silencing of α6 and α3 integrin (siA3 + siA6), inhibited the siα3 dependent increase in cell migration ($^{**}p < 0.005$). Both the induced (siA3) and constitutive migration (siCON) was dependent on β1 integrin as shown by AIIB2 antibody treatment (Fig. 5).

Internalized α6, β4 and α3 integrin was targeted to early endosomes

The endocytic fate of the internalized integrins was determined by staining cells with markers for key endocytic vesicular compartments. α6 integrin co-localized with early endosome marker, early endosome antigen 1 (EEA1) in untreated DU145 cells (Fig. 6A, C). The co-localization increased significantly in cells depleted of α3 integrin expression (siA3) (Fig. 6B–D, Pearson's Coefficient of Colocalization (Pr) increased from 0.28 to 0.36). Approximately 10% of EEA1 positive vesicles contained α6 integrin in untreated cells. Depletion of α3 integrin led to a 40% increase in α6 positive EEA1 vesicles (Fig. 6D). These early endosomes had specific domains positive for either EEA1 (green) or α6 integrin (red) or EEA1/α6 integrin overlapped regions (yellow) (Fig. 6C). The increase in α6 integrin in EEA1 vesicles was consistent with the increased intracellular accumulation of α6 integrin observed in the internalization assays (Fig. 2). There was no change in α6 integrin localization to Lamp1 vesicles in untreated or siα3 cells (Fig. 6 A, B, D), indicating that the internalized integrin was not targeted for degradation.

Since α6 integrin was observed redistributed to EEA1 and cell-cell locations upon depletion of α3 integrin expression (Fig. 6) and α6 can partner with either β1 or β4, we determined the localization of the β4 integrin under these same conditions. Integrin α6 and β4 localized to EEA1 vesicles in untreated DU145 cells (Fig. 7A, C). The co-localization with EEA1 increased significantly in cells depleted of α3 integrin expression (siA3) (Fig. 7B–D). Pearson's Coefficient of Colocalization (Pr) increased from 0.20 to 0.35 for α6 integrin; 0.25 to 0.46 for β4 integrin (Fig. 7D). Both α6 and β4 integrin increased within EEA1 vesicles (14 % to 34% for α6 integrin and 22% to 38% for β4 integrin) in response to silencing of α3 integrin expression (siA3) (Fig. 7D). Similar to the results in Figure 6, early endosomes were detected that had specific domains positive for either EEA1 (green), α6 integrin (red), β4 integrin (blue) or EEA1/α6/β4 integrin overlapped regions (white) (Fig. 7C). A discontinuous pattern of overlapping regions, as indicated by white pixels (Fig 7C, siA3, circles) was observed in α3 integrin silenced cells, suggesting distinct domains within

the endosome. Integrin α3 silenced cells showed a marked redistribution of α6β4 integrin to cell-cell locations (Fig. 6B, 7B).

Although α3 internalization rates were unaffected by the silenced expression of α6 integrin (Fig. 3), we determined whether the localization of α3 integrin was affected under these same conditions. Internalized integrin α3 showed significant co-localization with EEA1 in both untreated and α6 integrin silenced DU145 cells (siA6) (Fig. 8A, C). Pearson's Coefficient of Co-localization (Pr) remained unchanged (0.48 for untreated and 0.52 for siα6 integrin) (Fig. 8C). Under both conditions, approximately 50% of EEA1 vesicles were positive for α3 integrin (Fig 8C) and α3 integrin was not significantly associated with Lamp1 vesicles (Fig. 8B, C).

DISCUSSION

Internalization of cell surface integrins is a major regulator of their cell membrane expression and function and a prerequisite for integrin-mediated cancer cell migration [Desgrosellier and Cheresh, 2010]. Here we report internalization kinetics of laminin binding integrins using flow cytometry and first-order reaction kinetics model. The α6 integrin internalization rate was 3-fold higher as compared to α3 integrin, consistent with previous reports that the integrin alpha subunits have distinct internalization rates despite sharing the common integrin β1 partner [Bretscher, 1992; Winterwood et al., 2006]. For comparative purposes, an unrelated integrin (αvβ3 had a slower internalization rate than α6 integrin (2.20 min^{-1} versus 3.25 min^{-1}, respectively) whereas a growth-promoting receptor, the transferrin receptor, internalized with a rate of 15.08 min^{-1}.

Interestingly, the internalization rate does not necessarily reflect intracellular accumulation since the αvβ3 integrin has a slower internalization rate compared to α6 integrin (2.2 min^{-1} versus 3.25min^{-1}, respectively) but more internal accumulation compared to α6 integrin (65% versus 58%, respectively). Differences in accumulation likely reflect differences in recycling rate and adapter proteins for trafficking regulation. For example, Rab11-FIP1 (RCP) machinery is used by fibronectin/vitronectin binding integrins (αvβ3 and α5β1) [Caswell et al., 2008]. It remains to be determined which adapters are important for laminin binding integrins. The data also indicate that laminin binding integrins are internalized from the cell surface with significantly different rates from each other despite sharing the same β1 partner and the rates are distinct from non-laminin binding integrins and a growth-related receptor. Current experiments are underway to determine which Rab11 adapter proteins regulate α6 versus α3 integrin trafficking and recycling.

Integrins α3 and α6 work coordinately in normal cellular processes such as wound healing and epithelial development. In metastatic prostate cancer, distinct subtypes exist with differential expression of α3 and α6 integrins. High grade prostate carcinoma shows selective loss of α3 integrin while preserving expression of α6 integrin [Schmelz et al., 2002]. In model systems, α3 integrin expression can either prevent tumor progression or exacerbate it. In the current study, the presence of α3 integrin had a significant effect on internalization and cellular localization of α6 integrin. This could explain, in part, the previously discrepant reports since our results show that a coordination exists between α3

and α6 integrin. Here, depletion of α3 integrin led up to a 1.71-fold increase in α6 integrin internalization. The increased internalization of α6 integrin by silencing α3 integrin was accompanied by an increased migration on laminin. The results were consistent with previous studies utilizing an α3 integrin null mouse, where wound healing is faster owing to rapid and persistent keratinocyte migration dependent on α6 integrin [Margadant et al., 2009]. These results suggest a coordination of the laminin receptors may exist to influence cancer migration. Future studies will be important to determine which region of the α6 integrin is crucial for internalization in prostate cancer cells when α3 integrin is silenced. As specific regulators of α6 integrin internalization are found, it will be of interest to identify agonists and antagonists, as they may prove useful for blocking tumor metastasis via laminin lined structures. Silencing of α6 integrin expression did not alter the α3 integrin internalization rate, although an increased intracellular accumulation was observed. The data suggest a “unidirectional” regulation of internalization of laminin binding integrins. This is distinct from a previously reported reciprocal relationship between the recycling of fibronectin receptors α5β1 and αvβ3, where inhibition of either integrin promoted the recycling of the non-targeted integrin [Caswell et al., 2008].

The internalized α6 integrin was targeted to the early endosomes, which was markedly increased on silencing α3 integrin. An interesting observation was that the endosomes had specific domains of the cargo integrin, as suggested by discontinuous overlap with EEA1 distribution (Figs 6C, 7C and 8A). Integrin β4 was also found in these early endosomes. Importantly, α3 integrin depletion led to a redistribution of α6β4 to the plasma membrane at cell-cell contacts. This adds new interesting information that α6β4 integrin heterodimer localization is reminiscent of suprabasal distribution observed in the epidermis and results in enhanced tumorigenesis [Owens et al., 2003]. This may possibly be due to the recycling of the internalized integrins from early endosomes to the cell-cell lateral membrane. In human keratinocytes, α6 integrin has been observed in vesicles close to the lateral membrane, as well as in intercellular spaces by electron microscopy [Poumay et al., 1993]. Trafficking of α6 integrin to cell-cell lateral membrane has also been reported during epidermal development in zebrafish [Sonawane et al., 2009]. Integrins at cell-cell membrane have been implicated in cell-cell adhesion [Chattopadhyay et al., 2003; Emsley and Hagg, 2003] through the extracellular matrix present between cells [Behrendtsen et al., 1995]. Future work will determine if α6β4 integrin may be important for cell-cell interaction and promote collective cell migration, a characteristic of human prostate cancer invasion and metastasis [Nagle and Cress, 2011].

Supplementary Material

Refer to Web version on PubMed Central for supplementary material.

Acknowledgments

Research was supported in part by NIH research grants R01 CA 159406, CA 23074 and T32CA09213 and the Diane and Tim Bowden Scholarship Award. We acknowledge the support from Flow Cytometry Shared Resource (FCSR) at the University of Arizona Cancer Center. Many thanks to Dr. Greg Rogers and the members of the Rogers Lab for use of Deltavision deconvolution microscope.

References

Barczyk M, Carracedo S, Gullberg D. Integrins. Cell Tissue Res. 2010; 339:269–80. [PubMed: 19693543]

Behrendtsen O, Alexander CM, Werb Z. Cooperative interactions between extracellular matrix, integrins and parathyroid hormone-related peptide regulate parietal endoderm differentiation in mouse embryos. Development. 1995; 121:4137–48. [PubMed: 8575314]

Bretscher MS. Circulating integrins: alpha 5 beta 1, alpha 6 beta 4 and Mac-1, but not alpha 3 beta 1, alpha 4 beta 1 or LFA-1. EMBO J. 1992; 11:405–10. [PubMed: 1531629]

Bridgewater RE, Norman JC, Caswell PT. Integrin trafficking at a glance. J Cell Sci. 2012; 125:3695–701. [PubMed: 23027580]

Caswell PT, Chan M, Lindsay AJ, McCaffrey MW, Boettiger D, Norman JC. Rab-coupling protein coordinates recycling of alpha5beta1 integrin and EGFR1 to promote cell migration in 3D microenvironments. J Cell Biol. 2008; 183:143–55. [PubMed: 18838556]

Chattopadhyay N, Wang Z, Ashman LK, Brady-Kalnay SM, Kreidberg JA. alpha3beta1 integrin-CD151, a component of the cadherin-catenin complex, regulates PTPmu expression and cell-cell adhesion. J Cell Biol. 2003; 163:1351–62. [PubMed: 14691142]

Cress AE, Rabinovitz I, Zhu W, Nagle RB. The alpha 6 beta 1 and alpha 6 beta 4 integrins in human prostate cancer progression. Cancer Metastasis Rev. 1995; 14:219–28. [PubMed: 8548870]

De Arcangelis A, Mark M, Kreidberg J, Sorokin L, Georges-Labouesse E. Synergistic activities of alpha3 and alpha6 integrins are required during apical ectodermal ridge formation and organogenesis in the mouse. Development. 1999; 126:3957–68. [PubMed: 10433923]

Demetriou MC, Cress AE. Integrin clipping: a novel adhesion switch? J Cell Biochem. 2004; 91:26–35. [PubMed: 14689578]

Demetriou MC, Kwei KA, Powell MB, Nagle RB, Bowden GT, Cress AE. Integrin A6 Cleavage in Mouse Skin Tumors. Open Cancer J. 2008; 2:1–4. [PubMed: 20664806]

Desgrosellier JS, Cheresh DA. Integrins in cancer: biological implications and therapeutic opportunities. Nat Rev Cancer. 2010; 10:9–22. [PubMed: 20029421]

DiPersio CM, Hodivala-Dilke KM, Jaenisch R, Kreidberg JA, Hynes RO. alpha3beta1 Integrin is required for normal development of the epidermal basement membrane. J Cell Biol. 1997; 137:729–42. [PubMed: 9151677]

Emsley JG, Hagg T. alpha6beta1 integrin directs migration of neuronal precursors in adult mouse forebrain. Exp Neurol. 2003; 183:273–85. [PubMed: 14552869]

Frank SB, Miranti CK. Disruption of prostate epithelial differentiation pathways and prostate cancer development. Front Oncol. 2013; 3:273. [PubMed: 24199173]

Georges-Labouesse E, Messaddeq N, Yehia G, Cadalbert L, Dierich A, Le Meur M. Absence of integrin alpha 6 leads to epidermolysis bullosa and neonatal death in mice. Nat Genet. 1996; 13:370–3. [PubMed: 8673141]

Goldenring JR. A central role for vesicle trafficking in epithelial neoplasia: intracellular highways to carcinogenesis. Nat Rev Cancer. 2013; 13:813–20. [PubMed: 24108097]

Goldfinger LE, Hopkinson SB, deHart GW, Collawn S, Couchman JR, Jones JC. The alpha3 laminin subunit, alpha6beta4 and alpha3beta1 integrin coordinately regulate wound healing in cultured epithelial cells and in the skin. J Cell Sci. 1999; 112(Pt 16):2615–29. [PubMed: 10413670]

Hood JD, Cheresh DA. Role of integrins in cell invasion and migration. Nat Rev Cancer. 2002; 2:91–100. [PubMed: 12635172]

Hynes RO. Integrins: bidirectional, allosteric signaling machines. Cell. 2002; 110:673–87. [PubMed: 12297042]

Landowski TH, Gard J, Pond E, Pond GD, Nagle RB, Geffre CP, Cress AE. Targeting integrin alpha6 stimulates curative-type bone metastasis lesions in a xenograft model. Mol Cancer Ther. 2014; 13:1558–66. [PubMed: 24739392]

Longmate WM, Dipersio CM. Integrin Regulation of Epidermal Functions in Wounds. Adv Wound Care (New Rochelle). 2014; 3:229–246. [PubMed: 24669359]

Marchetti G, De Arcangelis A, Pfister V, Georges-Labouesse E. alpha6 integrin subunit regulates cerebellar development. Cell Adh Migr. 2013; 7:325–32. [PubMed: 23722246]

Margadant C, Raymond K, Kreft M, Sachs N, Janssen H, Sonnenberg A. Integrin alpha3beta1 inhibits directional migration and wound re-epithelialization in the skin. J Cell Sci. 2009; 122:278–88. [PubMed: 19118220]

Mitchell K, Svenson KB, Longmate WM, Gkirtzimanaki K, Sadej R, Wang X, Zhao J, Eliopoulos AG, Berditchevski F, Dipersio CM. Suppression of integrin alpha3beta1 in breast cancer cells reduces cyclooxygenase-2 gene expression and inhibits tumorigenesis, invasion, and cross-talk to endothelial cells. Cancer Res. 2010; 70:6359–67. [PubMed: 20631072]

Nagle RB, Cress AE. Metastasis Update: Human Prostate Carcinoma Invasion via Tubulogenesis. Prostate Cancer. 2011; 2011:249290. [PubMed: 21949592]

Owens DM, Romero MR, Gardner C, Watt FM. Suprabasal alpha6beta4 integrin expression in epidermis results in enhanced tumourigenesis and disruption of TGFbeta signalling. J Cell Sci. 2003; 116:3783–91. [PubMed: 12902406]

Park JW, Lee JK, Phillips JW, Huang P, Cheng D, Huang J, Witte ON. Prostate epithelial cell of origin determines cancer differentiation state in an organoid transformation assay. Proc Natl Acad Sci U S A. 2016; 113:4482–7. [PubMed: 27044116]

Ports MO, Nagle RB, Pond GD, Cress AE. Extracellular engagement of alpha6 integrin inhibited urokinase-type plasminogen activator-mediated cleavage and delayed human prostate bone metastasis. Cancer Res. 2009; 69:5007–14. [PubMed: 19491258]

Poumay Y, Leclercq-Smekens M, Grailly S, Degen A, Leloup R. Specific internalization of basal membrane domains containing the integrin alpha 6 beta 4 in dispase-detached cultured human keratinocytes. Eur J Cell Biol. 1993; 60:12–20. [PubMed: 8462591]

Ramsay AG, Marshall JF, Hart IR. Integrin trafficking and its role in cancer metastasis. Cancer Metastasis Rev. 2007; 26:567–78. [PubMed: 17786537]

Schmelz M, Cress AE, Scott KM, Burger F, Cui H, Sallam K, McDaniel KM, Dalkin BL, Nagle RB. Different phenotypes in human prostate cancer: alpha6 or alpha3 integrin in cell-extracellular adhesion sites. Neoplasia. 2002; 4:243–54. [PubMed: 11988844]

Schmelz M, Moll R, Hesse U, Prasad AR, Gandolfi JA, Hasan SR, Bartholdi M, Cress AE. Identification of a stem cell candidate in the normal human prostate gland. Eur J Cell Biol. 2005; 84:341–54. [PubMed: 15819412]

Shimizu O, Shiratsuchi H, Ueda K, Oka S, Yonehara Y. Alteration of the actin cytoskeleton and localisation of the alpha6beta1 and alpha3 integrins during regeneration of the rat submandibular gland. Arch Oral Biol. 2012; 57:1127–32. [PubMed: 22410146]

Sonawane M, Martin-Maischein H, Schwarz H, Nusslein-Volhard C. Lgl2 and E-cadherin act antagonistically to regulate hemidesmosome formation during epidermal development in zebrafish. Development. 2009; 136:1231–40. [PubMed: 19261700]

Sroka IC, Anderson TA, McDaniel KM, Nagle RB, Gretzer MB, Cress AE. The laminin binding integrin alpha6beta1 in prostate cancer perineural invasion. J Cell Physiol. 2010; 224:283–8. [PubMed: 20432448]

Sroka IC, Chen ML, Cress AE. Simplified purification procedure of laminin-332 and laminin-511 from human cell lines. Biochem Biophys Res Commun. 2008; 375:410–3. [PubMed: 18713621]

Sroka TC, Marik J, Pennington ME, Lam KS, Cress AE. The minimum element of a synthetic peptide required to block prostate tumor cell migration. Cancer Biol Ther. 2006; 5:1556–62. [PubMed: 17102593]

Stipp CS. Laminin-binding integrins and their tetraspanin partners as potential antimetastatic targets. Expert Rev Mol Med. 2010; 12:e3. [PubMed: 20078909]

Strachan LR, Condic ML. Cranial neural crest recycle surface integrins in a substratum-dependent manner to promote rapid motility. J Cell Biol. 2004; 167:545–54. [PubMed: 15520227]

Teckchandani A, Toida N, Goodchild J, Henderson C, Watts J, Wollscheid B, Cooper JA. Quantitative proteomics identifies a Dab2/integrin module regulating cell migration. J Cell Biol. 2009; 186:99–111. [PubMed: 19581412]

van der Neut R, Krimpenfort P, Calafat J, Niessen CM, Sonnenberg A. Epithelial detachment due to absence of hemidesmosomes in integrin beta 4 null mice. Nat Genet. 1996; 13:366–9. [PubMed: 8673140]

Varzavand A, Drake JM, Svensson RU, Herndon ME, Zhou B, Henry MD, Stipp CS. Integrin alpha3beta1 regulates tumor cell responses to stromal cells and can function to suppress prostate cancer metastatic colonization. Clin Exp Metastasis. 2013; 30:541–52. [PubMed: 23224938]

Watt FM. Role of integrins in regulating epidermal adhesion, growth and differentiation. EMBO J. 2002; 21:3919–26. [PubMed: 12145193]

Werb Z, Tremble PM, Behrendtsen O, Crowley E, Damsky CH. Signal transduction through the fibronectin receptor induces collagenase and stromelysin gene expression. J Cell Biol. 1989; 109:877–89. [PubMed: 2547805]

Wiley HS, Cunningham DD. The endocytotic rate constant. A cellular parameter for quantitating receptor-mediated endocytosis. J Biol Chem. 1982a; 257:4222–9. [PubMed: 6279628]

Wiley HS, Cunningham DD. The endocytotic rate constant. A cellular parameter for quantitating receptor-mediated endocytosis. Journal of Biological Chemistry. 1982b; 257:4222–4229. [PubMed: 6279628]

Winterwood NE, Varzavand A, Meland MN, Ashman LK, Stipp CS. A critical role for tetraspanin CD151 in alpha3beta1 and alpha6beta4 integrin-dependent tumor cell functions on laminin-5. Mol Biol Cell. 2006; 17:2707–21. [PubMed: 16571677]

Witkowski CM, Rabinovitz I, Nagle RB, Affinito KS, Cress AE. Characterization of integrin subunits, cellular adhesion and tumorgenicity of four human prostate cell lines. J Cancer Res Clin Oncol. 1993; 119:637–44. [PubMed: 7688749]

Yoon S-O, Shin S, Mercurio AM. Hypoxia Stimulates Carcinoma Invasion by Stabilizing Microtubules and Promoting the Rab11 Trafficking of the α6β4 Integrin. Cancer Research. 2005; 65:2761–2769. [PubMed: 15805276]

Zhou B, Gibson-Corley KN, Herndon ME, Sun Y, Gustafson-Wagner E, Teoh-Fitzgerald M, Domann FE, Henry MD, Stipp CS. Integrin alpha3beta1 can function to promote spontaneous metastasis and lung colonization of invasive breast carcinoma. Mol Cancer Res. 2014; 12:143–54. [PubMed: 24002891]

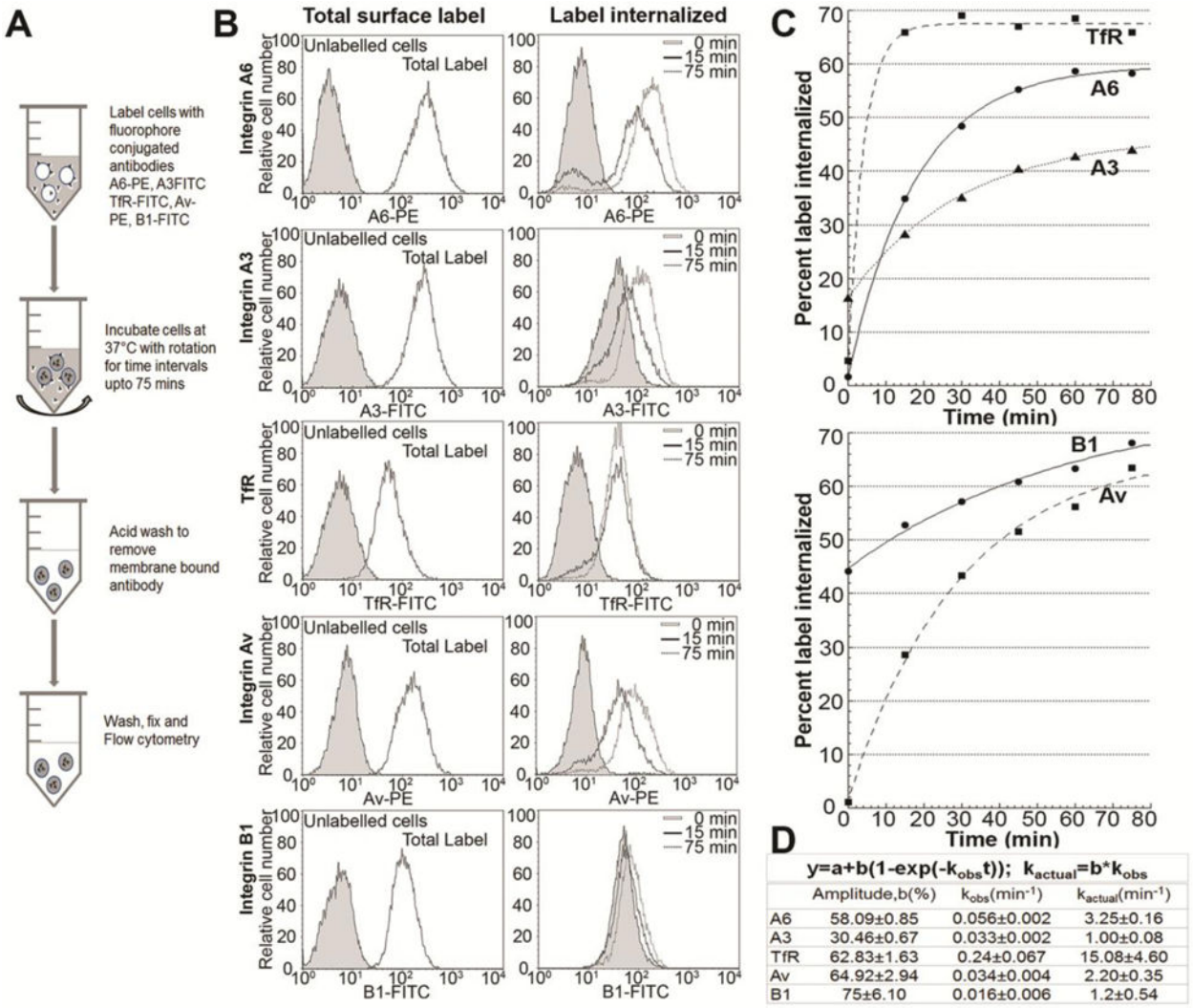

Figure 1. Internalization kinetics of integrin subunits and transferrin receptor

[A] Schematic representation of the internalization assay. DU145 cells were surface labelled with fluorophore conjugated antibodies against integrin subunits α6 (A6-PE), α3 (A3-FITC), αv (Av-PE), β1 (B1-FITC), or transferrin receptor (TfR-FITC) at 4°C for 1 hr. followed by internalization at 37°C for different time intervals. Remaining surface label was removed and cells were fixed and analyzed by flow cytometry. **[B]** Flow histograms of receptor internalization. Left panel shows total surface levels of the indicated receptor and unlabeled cells (shaded) are shown as control. Right panel shows histogram profile of the labelled receptor internalized at representative time intervals showing increase in mean peak fluorescence with increase in time of internalization. **[C]** Internalization curve of the receptors. Percent of label internalized (calculated as percent mean peak fluorescence of internalized label at a given time point versus total surface label) is plotted against time of internalization. First order curve is fitted using Kaleidagraph (R^2>0.98). **[D]** Parameters of internalization kinetics: maximum intracellular accumulation (amplitude, b) and internalization rate constants (observed, k_{obs} and actual, k_{actual}) calculated using first order

rate kinetics. Histograms and kinetic curves are representative of at least 3 independent experiments.

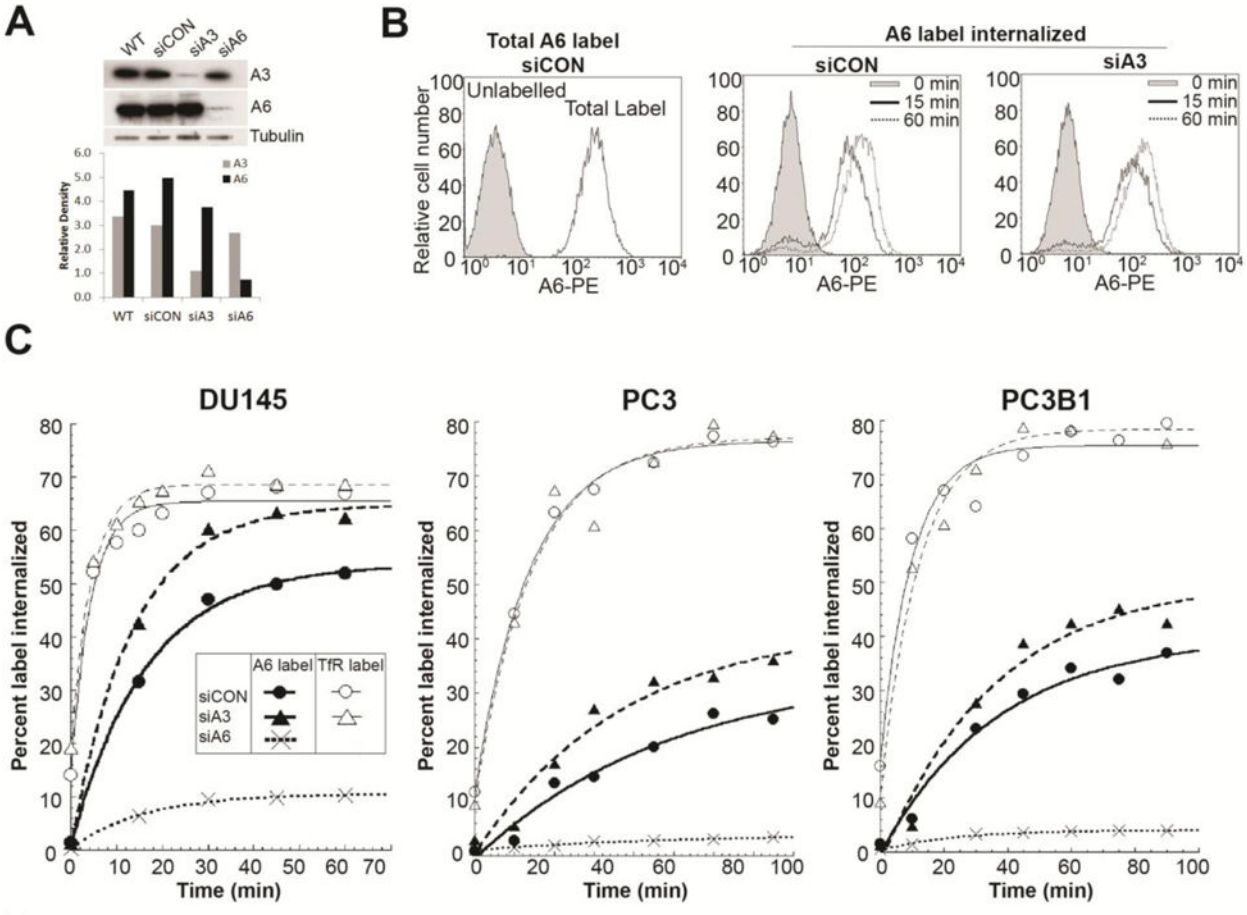

D

$y=a+b(1-\exp(-k_{obs}t))$; $k_{actual}=b*k_{obs}$

		DU145			PC3			PC3B1		
		Amplitude, b(%)	k_{obs}(min^{-1})	k_{actual}(min^{-1})	Amplitude, b(%)	k_{obs}(min^{-1})	k_{actual}(min^{-1})	Amplitude, b(%)	k_{obs}(min^{-1})	k_{actual}(min^{-1})
Integrin α6	siCON	52.48±2.09	0.061±0.006	3.20±0.44	34.61±2.15	0.020±0.010	0.69±0.19	40.32±4.2	0.026±0.001	1.04±0.14
	siA3	63.83±3.03	0.074±0.009	4.72±0.79*	42.1±2.05	0.028±0.011	1.18±0.32*	52.36±6.72	0.028±0.009	1.47±0.65*
TfR	siCON	65.48±3.30	0.226±0.037	14.79±3.16	76.52±2.0	0.072±0.005	5.51±0.52	75.4±5.22	0.1±0.022	7.54±2.18
	siA3	68.64±2.05	0.221±0.023	15.16±2.03	77.41±3.3	0.070±0.016	5.40±1.47	78.39±3.91	0.092±0.01	7.21±1.14

Figure 2. Internalization of integrin α6 after silencing integrin α3 expression

DU145, PC3 or PC3B1 cells were transfected with non-targeting siRNA (SiCON), siRNA against α3 integrin (siA3), or α6 integrin (siA6). **[A]** Immunoblot showing integrin α6 (AA6NT) and integrin α3 (AB1920) expression in untreated (WT), siCON, siA3, siA6 DU145 cells. **[B]** Internalization assay for integrin α6 and TfR were performed on siCON and siA3 cells. Flow histogram of total labelled integrin α6 at the surface and amount internalized at different time intervals in siCON and siA3 treated DU145 cells. **[C]** Internalization curve of α6 integrin (A6) in siCON, siA3, and siA6 cells and transferrin receptor (TfR) in siCON, siA3 treated DU145, PC3 and PC3B1 cells. Percent label internalized was calculated and first order kinetic curve was fitted as previously described in figure 1. **[D]** Maximum intracellular accumulation (amplitude, b) and internalization rate constants (observed, k_{obs} and actual, k_{actual}) calculated as per first order rate kinetics.

Results represent 4 independent experiments. Statistical significance calculated for change in k_{actual} of siA3 versus siCON cells as per student's t test, unpaired, *$p < 0.05$, $n = 4$.

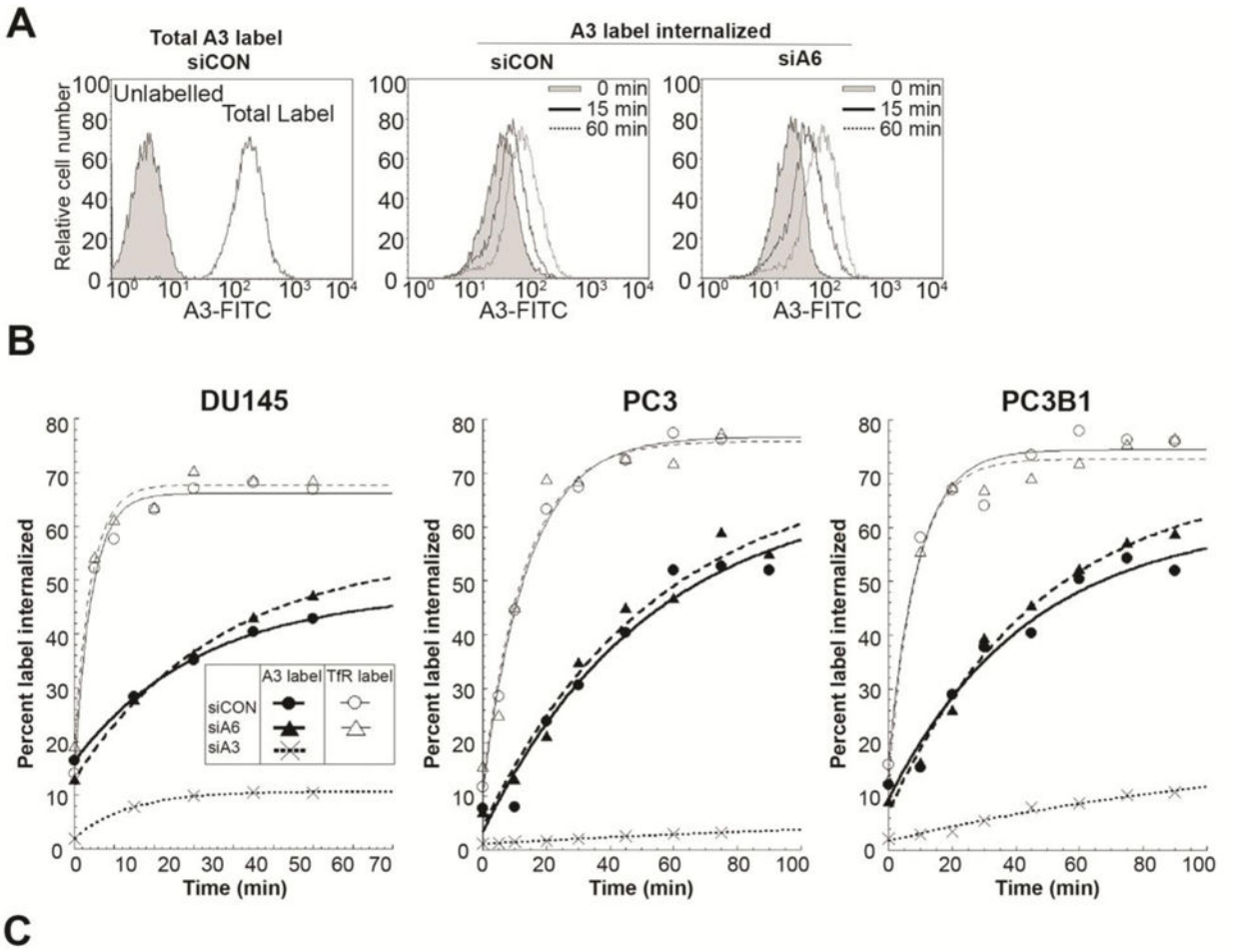

C

$y=a+b(1-\exp(-k_{obs}t))$; $k_{actual}=b*k_{obs}$

		DU145			PC3			PC3B1		
		Amplitude, b(%)	k_{obs}(min^{-1})	k_{actual}(min^{-1})	Amplitude, b(%)	k_{obs}(min^{-1})	k_{actual}(min^{-1})	Amplitude, b(%)	k_{obs}(min^{-1})	k_{actual}(min^{-1})
Integrin α3	siCON	31.27±1.02	0.033±0.002	1.03±0.09	63.77±11.74	0.018±0.008	1.20±0.73	51.84±6.6	0.023±0.007	1.19±0.51
	siA6	42.11±1.59	0.027±0.002	1.13±0.12	66.67±10.93	0.018±0.006	1.22±0.60	62.18±5.14	0.021±0.004	1.30±0.35
TfR	siCON	65.72±2.94	0.234±0.036	15.37±3.05	76.78±1.94	0.070±0.005	5.43±0.52	74.41±5.22	0.108±0.022	8.03±2.20
	siA6	66.12±2.98	0.230±0.033	15.21±2.86	75.98±5.2	0.074±0.015	5.62±1.52	72.65±5.06	0.117±0.019	8.50±1.97

Figure 3. Internalization kinetics of integrin α3 after silencing integrin α6 expression

Internalization assay for integrin α3 was performed on DU145 cells transfected with non-targeting siRNA (siCON), siRNA against α3 integrin (siA3), or α6 integrin (siA6). **[A]** Flow histogram of total labelled integrin α3 (A3) at the surface and amount internalized at different time intervals in siCON and siA6 treated DU145 cells. **[B]** Internalization curve of α3 integrin and transferrin receptor (TfR) in siCON, siA6, and siA3 treated DU145, PC3 and PC3B1 cells. **[C]** Maximum intracellular accumulation (amplitude, b) and internalization rate constants (observed, k_{obs} and actual, k_{actual}) calculated as per first order kinetics. Results represent 4 independent experiments.

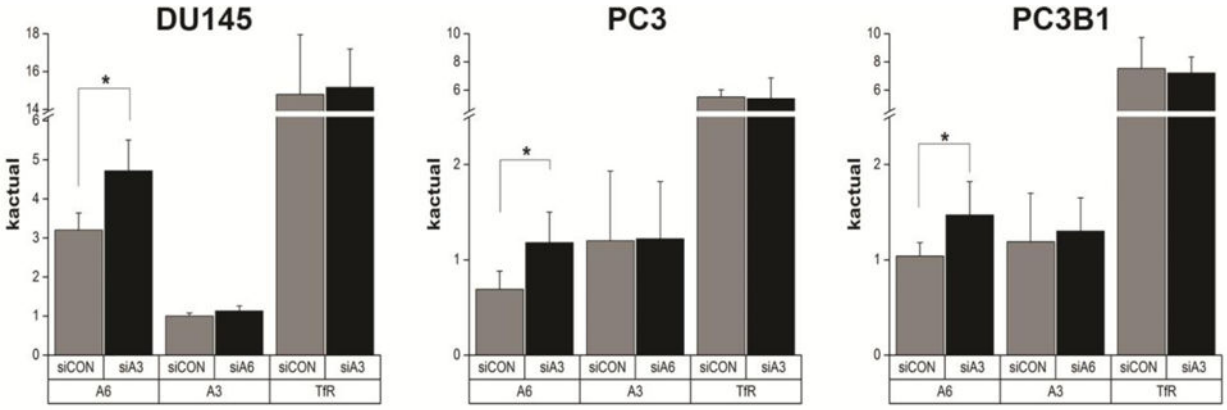

Figure 4. Actual internalization rate constant of laminin binding integrins on depletion of either subunit

Actual Internalization rate constant (k_{actual}) of α6, α3 or TfR internalization in DU145, PC3 and PC3B1 cells treated with siCON (grey bars), siA6 or siA3 treated cells (black bars). *$p < 0.05$, $n = 4$.

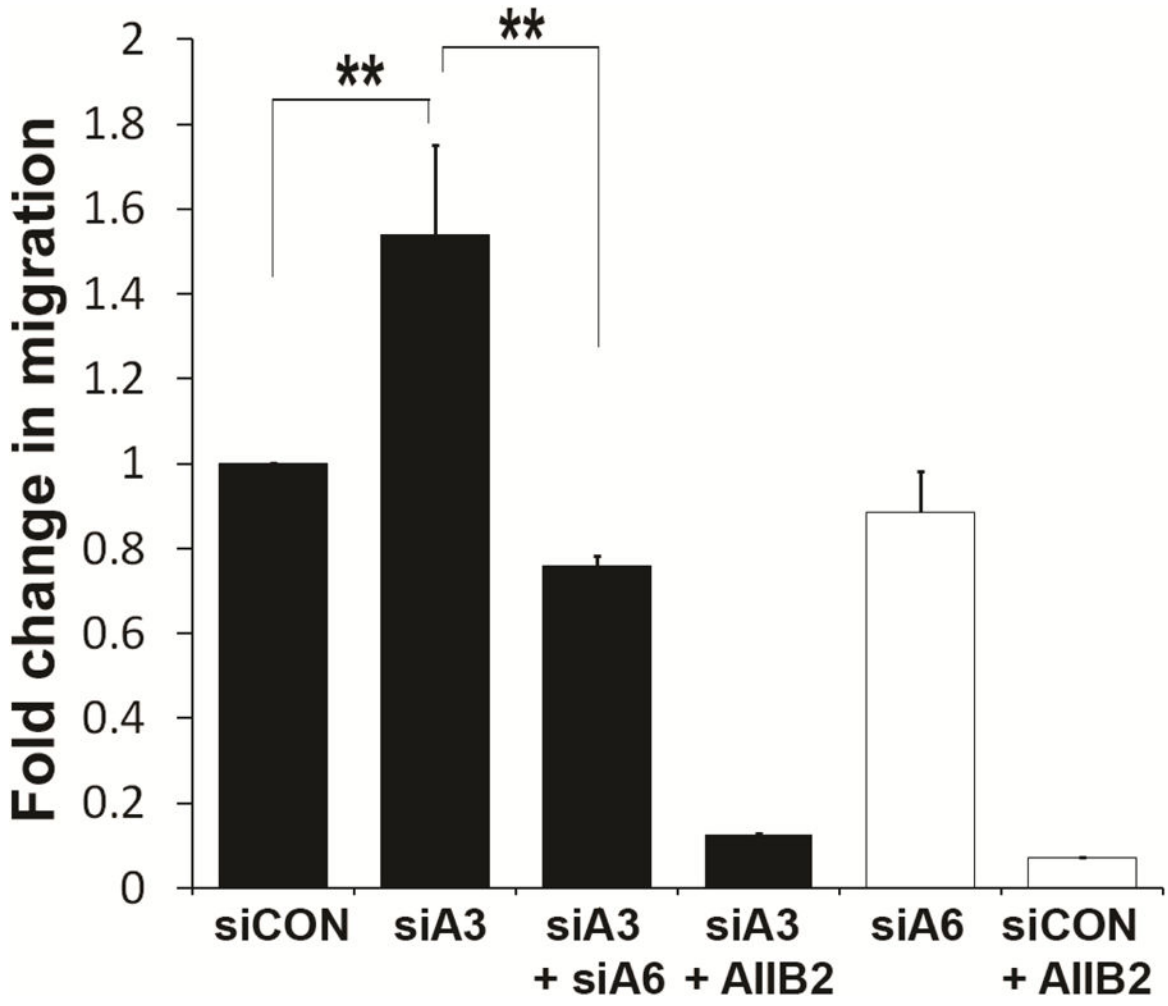

Figure 5. Depletion of α3 integrin increased cell migration dependent on α6β1 integrin

DU145 cells were treated with non-targeting siRNA (siCON), siRNA targeting α3 integrin (siA3), and/or α6 integrin (siA6) followed by modified Boyden chamber cell migration assay for 6 hours. Statistical significance assessed by student's unpaired t-test, (n = 3, each experiment in triplicates), **p < 0.005.

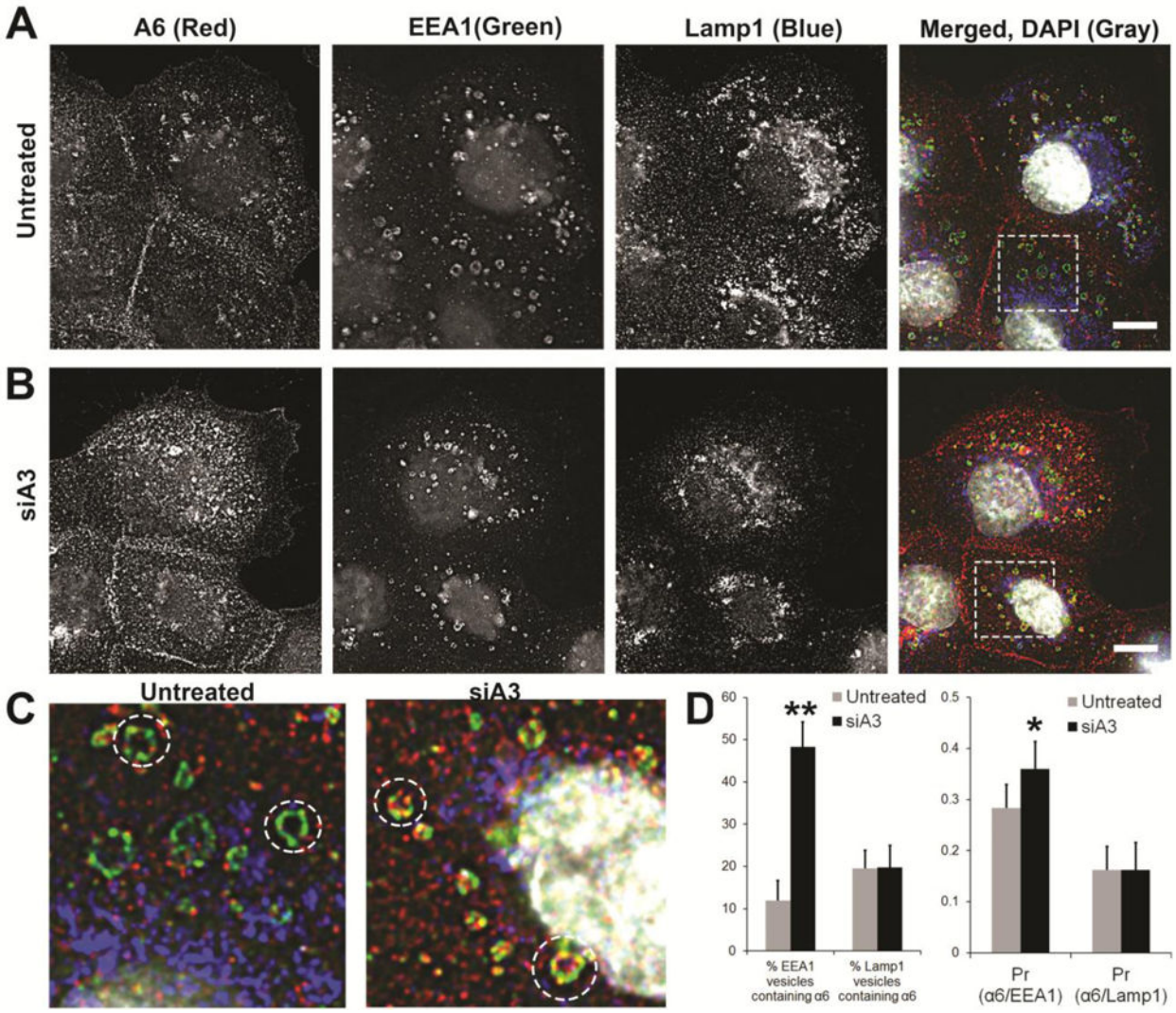

Figure 6. Distribution of α6 integrin in endosomal vesicles and redistribution on silencing α3 integrin expression

Surface integrin α6 was labelled with J1B5 in DU145 cells and allowed to internalize for 40 minutes in the presence of primaquine (a recycling inhibitor) to achieve maximum intracellular accumulation. Cells were fixed, permeabilized, and immunostained for markers of intracellular vesicular compartments. **[A]** Untreated DU145 cells, **[B]** siA3 treated cells. Integrin α6 (A6, red), early endosome antigen 1 (EEA1) positive early endosomes (green), Lamp1 vesicles (blue) and DAPI (gray) in merged image. Images acquired by confocal microscopy. **[C]** Magnified images of boxed sections are shown for untreated and siA3 treated DU145 cells. **[D]** Percent EEA1 or Lamp1 vesicles containing α6 integrin and mean Pearson coefficient of correlation of α6 integrin with EEA1 (Pr(α6/EEA1) or with Lamp1(α6/Lamp1) are reported for untreated or siA3 treated cells based on 10 different field of view in 3 independent experiments (*$p < 0.05$ **$p < 0.005$). Bars, 10μm.

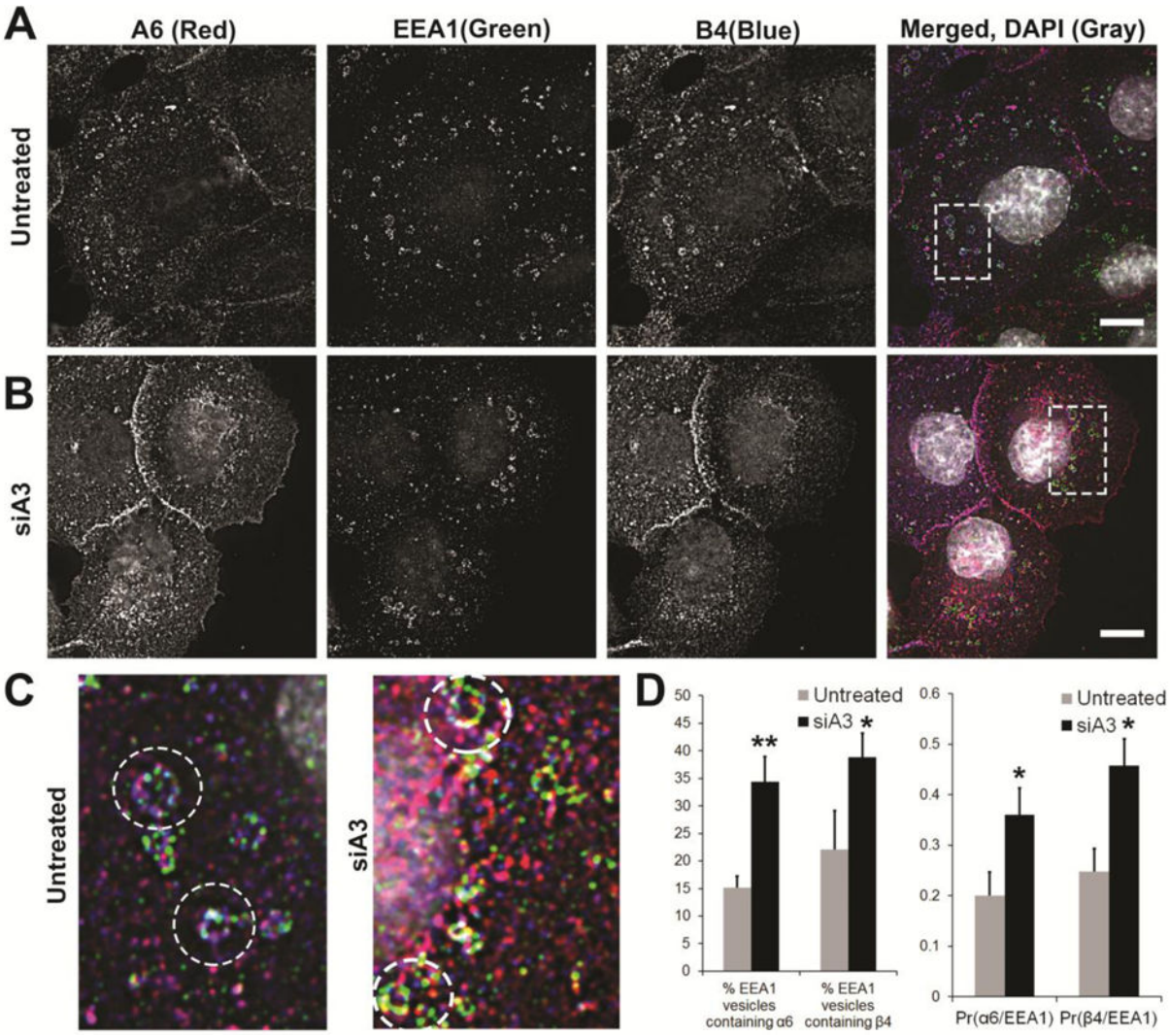

Figure 7. Distribution of α6β4 integrin in early endosomes on silencing α3 integrin expression

Surface α6 integrin was labelled with J1B5 and β4 integrin with ASC3 antibody in DU145 cells and allowed to internalize for 40 minutes in the presence of primaquine (a recycling inhibitor) to achieve maximum intracellular accumulation. Cells were fixed, permeabilized, and immunostained for markers of intracellular vesicular compartments. **[A]** Untreated DU145 cells, **[B]** siA3 treated cells. Integrin α6 (A6, red), early endosome antigen 1 (EEA1) positive early endosomes (green), integrin β4 (B4, blue) and DAPI (gray) in merged image. Images acquired by confocal microscopy. **[C]** Magnified images of boxed sections are shown for untreated and siA3 treated DU145 cells. **[D]** Percent EEA1 vesicles containing α6 or β4 integrin and mean Pearson coefficient of correlation of α6 integrin with EEA1 (Pr(α6/EEA1) or β4 with Lamp1(α6/EEA1) are reported for untreated or siA3 treated cells based on 10 different field of view in 3 independent experiments (*$p < 0.05$ **$p < 0.005$). Bars, 10μm.

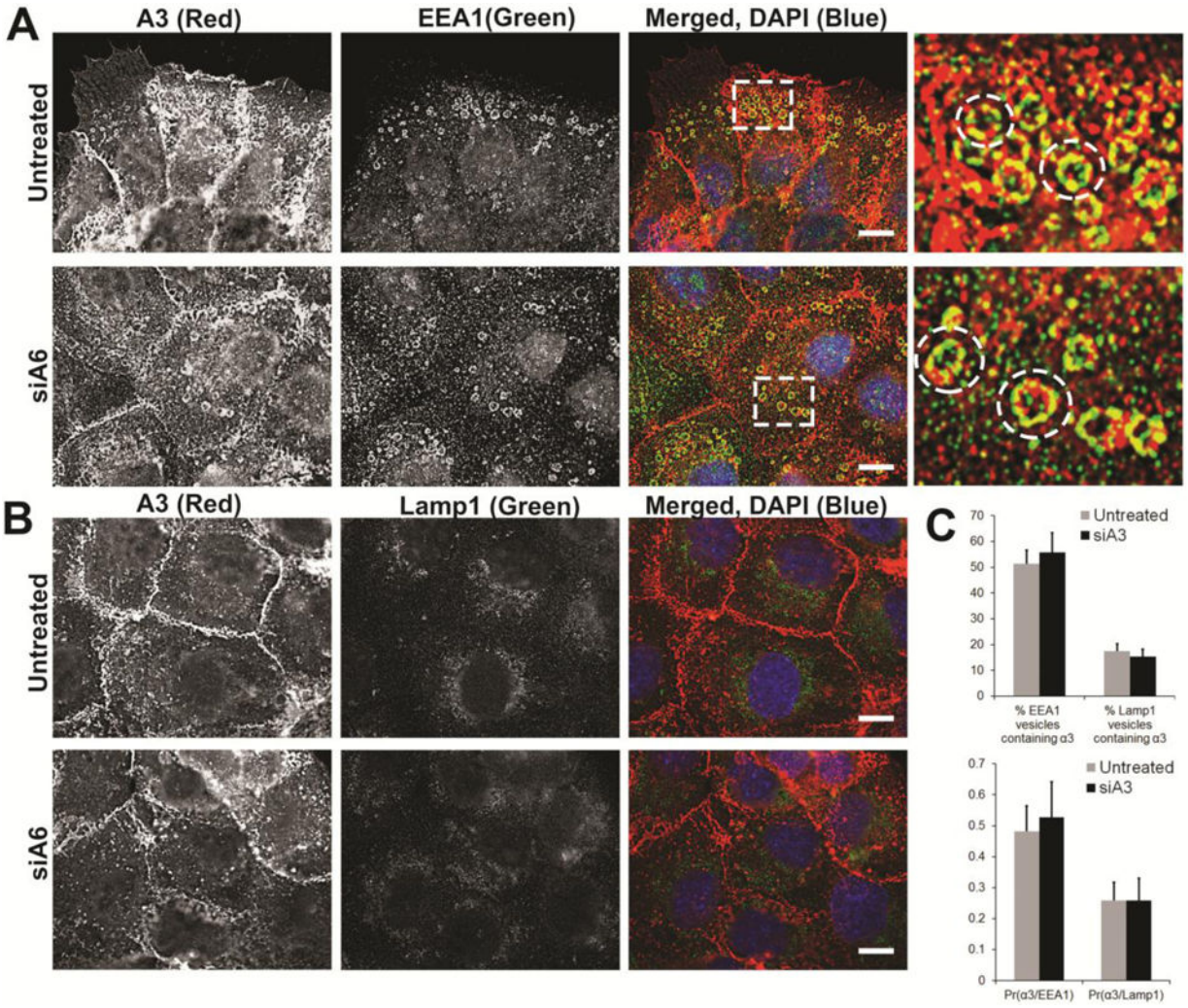

Figure 8. Distribution of α3 integrin in endosomal vesicles on silencing α6 integrin expression

P1B5 labelled surface integrin α3 in DU145 cells was allowed to internalize for 40 minutes in the presence of primaquine (a recycling inhibitor) to achieve maximum intracellular accumulation. Cells were fixed, permeabilized, and immunostained for markers of intracellular vesicular compartments. Untreated and siA6 treated DU145 cells stained for integrin α3 (A3, red) with early endosome antigen 1 (EEA1, green) in merged image **[A]** or Lamp1 (green) **[B]** and DAPI (blue). Magnified image of the boxed region are shown to demonstrate co-localization. Images acquired by confocal microscopy. **[C]** Percent EEA1 or Lamp1 vesicles containing α3 integrin and mean Pearson coefficient of correlation of α3 integrin with EEA1 (Pr(α3/EEA1) or with Lamp1(α3/Lamp1) are reported for untreated or siA6 treated cells based on 10 different field of view in 3 independent experiments. Bars, 10μm.